was to eliminate b and l as variables by choosing a particular geometry. The gravitational force was then varied and the critical velocity $\mathbf{u}$ was found experimentally. Only favorable gravitational forces (those directed from the gas to the liquid) were used since unfavorable gravitational forces tend to dominate the stability equation. In practical situations the pressure gradient is usually favorable during the firing of the rocket when fuel is being used.

Experimental Results

Shown in Fig. 3 are the results of the investigation of the stability of the interface in the rectangular channel for two different plate spacings. The average interface velocity was obtained by measuring the distance and time required for the gas-liquid interface to move from the starting position to the tank outlet. The solid lines represent the predictions of Eq. (3) for the conditions of the experiment and for an infinite tank. The three states of the interface have been labeled stable, neutral, and unstable. The stable interface condition existed when the interface remained flat with very little penetration of the gas into the liquid, while the neutral case had moderate penetration of the gas. The unstable case represents large penetration of fingers[2] into the liquid fuel.

Agreement of the data points and theory is seen to be good. The major difference is due to the large neutral region, and is the result of funnelling pressure gradients caused by the finite tank geometry. The neutral region was larger for the low-gravity tests where funnelling would be more influential. For the tests with higher gravitational forces (0.01 g) the experimental results were dominated by the gravitational forces, and the region of neutral stability became very small. Changing the plate spacing b did not cause any observable qualitative changes in the comparison between theory and experiment, and the correct quantitative changes were predicted by Eq. (3). All the tests were carried out at a creeping flow Reynolds numbers[1] for which the Hele-Shaw assumptions were justified.

The major source of experimental error was due to small inaccuracies in the leveling of the channel in the direction transverse to the flow. This error resulted in a tendency of the fluid to flow slightly down one side of the channel more than the other. The maximum magnitude of the transverse gravitational field at any point in the channel was 0.001 g, and the influence of this field was the greatest for the very low-gravity tests.

Another important characteristic of a fuel tank system is the amount of fluid left in the tank after the driver gas reaches the exit. Figure 4 shows the results of the measurement of the percentage of fluid left remaining in the system. The tests were carried out with three outlet geometries in order to determine the influence of funnelling on the data. These outlet geometries consisted of the following: a) no exit constriction; b) single row of spacers in the exit; and c) a large rounded plug in the exit. It was found that both the spacers and the plug improved the performance of the Hele-Shaw cell. The greatest improvement occurred with the large plug in the exit and this indicates that funnelling can be reduced, since the plug changes the exit pressure distribution. The exit spacers also reduced the amount of fluid left in the tank, and this was a result of increased surface tension in the exit. For low velocity ($V > 2$ cm/sec) and moderate gravitational force ($g > 0.005$) it was found that the percent of fluid left in the tank could be kept under 5%, which is a respectable result.

Conclusions

The major conclusions of this investigation are the following: 1) Hele-Shaw and porous medium fuel tank flow systems are feasible, and may represent an effective way of controlling sloshing in low gravity environments; 2) funnelling may be reduced considerably by changing the outlet drain configuration of the Hele-Shaw channel; 3) almost full recovery of the liquid fuel may be obtained by keeping the interface velocity below the interface stability limit; 4) the influence of surface tension is to stabilize the gas-liquid interface in the Hele-Shaw channel. It is not yet clear how surface tension will influence porous medium tanks.

References

[1] Schlichting, H., *Boundary Layer Theory*, 6th ed., McGraw-Hill, New York, 1968, pp. 104–116.

[2] Saffman, P. G. and Taylor, G. I., "The Penetration of a Fluid into a Porous Medium or Hele-Shaw Cell Containing a More Viscous Liquid," *Proceedings of the Royal Society of London, Ser. A*, 1958, pp. 245, 312–329.

Leading Characteristic in Conical Nozzle Flows and the Effect of Manufacturing Errors

Roy Scott Hickman*
University of California at Santa Barbara, Santa Barbara, Calif.

CONICAL expansion nozzles followed by contoured nozzles are of use in any supersonic wind tunnel.[1] These shapes are attractive because of the availability of the nozzle contours developed by Cresci[2] and because of their relative ease of manufacture. In these nozzle contours it is assumed that a relatively long conical section (long with respect to the throat radius) has fully conical inviscid flow at its exit. Then a contour is generated using the theory of characteristics which will produce a final uniform Mach number and parallel flow.

It has been observed by Edenfield[1] that slight manufacturing errors produce relatively large overexpansions at the beginning of the recompression region, even when the influence of the boundary layer displacement thickness was accounted for. The displacement thickness correction was everywhere less than 3% of the local radius and was accounted for in the nozzle contour. The accuracy of displacement thickness prediction was approximately 10% or within 0.3% of the nozzle radius. Several nozzles were reported with progressively better allowances for displacement thickness. The purpose of this Note is to provide an estimate of effects of manufacturing errors on the overexpansion.

Along a characteristic ξ, we can write (see Fig. 1)

$$d\xi \cos(\mu - \theta) = dx$$

and

$$-d\xi \sin(\mu - \theta) = dy \tag{1}$$

where dx and dy are the changes in x and y along the ξ characteristic for a change in ξ of $d\xi$, μ is the Mach angle and θ is the local flow inclination to the axis. Then we can write

$$dy/dx = -\sin(\mu - \theta)/\cos(\mu - \theta) \tag{2}$$

where dy/dx is the slope of the ξ characteristic. For the hypersonic case in which μ and θ are both small,

$$dy/dx \simeq -(\mu - \theta) \tag{3}$$

where $\tan\theta \simeq \theta \simeq y/x$ for small θ and

$$\mu = \sin^{-1}(1/M) \simeq 1/M \text{ or } \mu \simeq c/u$$

Received October 28, 1969; revision received April 2, 1970.

* Associate Professor.

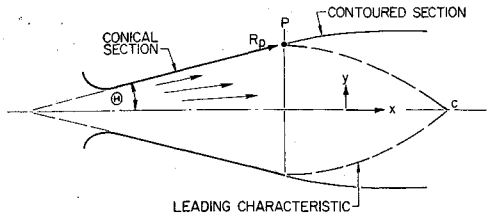

Fig. 1 Nozzle geometry.

where c and u are the local sound speed and velocity, respectively.

We are considering here the case of large Mach number so that u is close to its thermodynamic limit and may be treated as constant. Therefore, from continuity the density is

$$\rho \simeq \rho_p(r_p/r)^2 \tag{4}$$

Where the subscript p refers to the point where the leading characteristic starts, and r is the radial distance from the origin. Assuming an isentropic flow, $p \propto \rho^\gamma$, of perfect gas, $p \propto \rho T \propto \rho c^2$, we have

$$c = c_p(r_p/r)^{\gamma-1} \tag{5}$$

and using the fact that $x \simeq r$

$$\mu \simeq (r_p/x)^{\gamma-1}/M_P \tag{6}$$

and $M_P = u/c_p$. Equation (3) becomes

$$dy/dx = (y/x) - (1/x)^{\gamma-1}/M_P \tag{7}$$

where the variables have been made nondimensional by dividing by r_p. At $x = 1$, $y = \sin\Theta \simeq \Theta$, where Θ is the nozzle half angle. The solution to Eq. (7) is

$$y = \Theta x + (1/x^{\gamma-2} - x)/M_P(\gamma - 1) \tag{8}$$

and the point where the leading characteristic crosses the axis is the point at which $y \to 0$, i.e., at

$$x_c = 1/[1 - M_P(\gamma - 1)\Theta]^{1/(\gamma-1)} \tag{9}$$

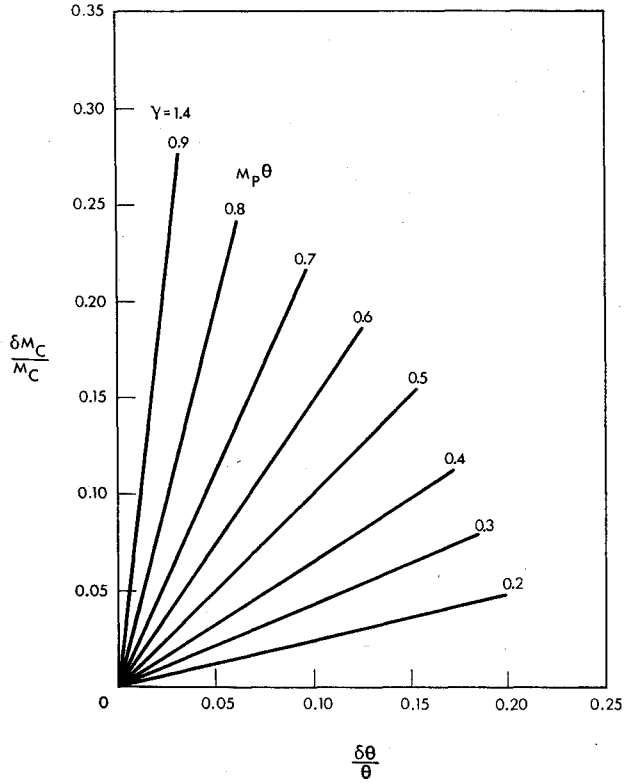

Fig. 2 Variation in Mach number uncertainty vs angular uncertainty.

The fractional error in x_c caused by an error in the product $M_P\Theta$ will be

$$\delta x_c/x_c \simeq \delta(M_P\Theta)/[1 - M_P(\gamma - 1)\Theta] \tag{10}$$

Clearly if M_P is large, a large error in x_c can occur for small manufacturing errors in Θ. The Mach number in the conical section varies as $1/\mu$ or

$$M_c = M_p(x_c)^{\gamma-1} \tag{11}$$

Assuming that M_P is large Eqs. (10) and (11) yield

$$\delta M_c/M_c \simeq (\gamma - 1)M_P\delta\Theta/[1 - (\gamma - 1)M_P\Theta] \tag{12}$$

The error in M_c is controlled by errors in the location of the junction between the conical-contoured sections and in the error in Θ. For the data presented by Edenfield,[1] $\delta M_c/M_c \simeq 15\%$ with $\Theta = 12°$, $M_P \simeq 7$, $R_P \simeq 8$ in. This error could be caused if $\delta\Theta = 0.24°$. This error in Θ corresponds to an error in the diameter at the cone exit of about 0.333 in. which is somewhat large for usual machine tolerance.

The sensitivity of Mach number uncertainty to angular uncertainty is plotted in Fig. 2.

References

[1] Edenfield, E. E., "Contoured Nozzle Design and Evaluation for Hot Shot Wind Tunnels," AIAA Paper 68-369, San Francisco, Calif., 1968.

[2] Cresci, R. F., "Tabulations of Coordinates for Hypersonic Axisymmetric Nozzles," Pt. I & II, TN 58-300, July 1960, Wright Air Development Center.

Experimental Investigation of a Luneberg Lens Antenna for Communications Satellites

Henning W. Scheel*
Ingenieurbüro Scheel, Berlin, Germany

Concept and Introduction

A LUNEBERG lens can be mounted at the end of a spin-stabilized synchronous satellite so that a small feed directed at the center of the lens can be rotated 360° around the lens. This feed is connected to the satellite receiver/transmitter by a coaxial cable and a rotating joint on the spin axis. The low-directive pattern of the feed is concentrated by the Luneberg lens to a narrow pencil beam. As the feed is counterrotated to the satellites spin motion by its own motor, this antenna beam can be locked on the earth or any specific place of it. Figure 1 is an outline drawing of the installed lens and feed arrangement.

Luneberg spheres are lenses that have a dielectric constant ϵ that obeys the following law:

$$\epsilon = n^2 = 2 - (r/a)^2$$

where n = refractive index, $D/2 = a$ = outer radius of lens, and r = radius to actual point; i.e., the dielectric constant in the center of the lens equals 2 and reduces to unity at the rim.

Presented as Paper 68-230 at the AIAA 2nd Communications Satellite Systems Conference, San Francisco, Calif., April 8–10, 1968; submitted July 22, 1968; revision received February 10, 1970. This work is supported in part by Bundesministerium für wissenschaftliche Forschung, Federal Republic of Germany, Contract RV 1—Na/08/66.

* Consulting Engineer.